RESEARCH ARTICLE

The biogeochemical role of *Actinobacteria* in Altamira Cave, Spain

Soledad Cuezva[1], Angel Fernandez-Cortes[2], Estefania Porca[3], Lejla Pašić[4], Valme Jurado[3], Mariona Hernandez-Marine[5], Penelope Serrano-Ortiz[6], Bernardo Hermosin[3], Juan Carlos Cañaveras[1], Sergio Sanchez-Moral[2] & Cesareo Saiz-Jimenez[3]

[1]Laboratorio de Petrologia Aplicada, Departamento de Ciencias de la Tierra y del Medio Ambiente, Universidad de Alicante, Alicante, Spain; [2]Museo Nacional de Ciencias Naturales, MNCN-CSIC, Madrid, Spain; [3]Instituto de Recursos Naturales y Agrobiologia, IRNAS-CSIC, Sevilla, Spain; [4]Department of Biology, Biotechnical Faculty, University of Ljubljana, Ljubljana, Slovenia; [5]Facultad de Farmacia, Universidad de Barcelona, Barcelona, Spain; and [6]Centro Andaluz de Medio Ambiente, Granada, Spain

Correspondence: Cesareo Saiz-Jimenez, Instituto de Recursos Naturales y Agrobiologia, IRNAS-CSIC, Av. Reina Mercedes 10, 41012 Sevilla, Spain. Tel.: +34 954624711; fax: +34 954624002; e-mail: saiz@irnase.csic.es

Received 21 October 2011; revised 6 April 2012; accepted 11 April 2012.
Final version published online 4 May 2012.

DOI: 10.1111/j.1574-6941.2012.01391.x

Editor : Christian Griebler

Keywords
calcium carbonate polymorphs; *Actinobacteria*; cave colonization; CO_2 uptake.

Abstract

The walls and ceiling of Altamira Cave, northern Spain, are coated with different coloured spots (yellow, white and grey). Electron microscopy revealed that the grey spots are composed of bacteria and bioinduced $CaCO_3$ crystals. The morphology of the spots revealed a dense network of microorganisms organized in well-defined radial and dendritic divergent branches from the central area towards the exterior of the spot, which is coated with overlying spheroidal elements of $CaCO_3$ and $CaCO_3$ nest-like aggregates. Molecular analysis indicated that the grey spots were mainly formed by an unrecognized species of the genus *Actinobacteria*. CO_2 efflux measurements in rocks heavily covered by grey spots confirmed that bacteria-forming spots promoted uptake of the gas, which is abundant in the cave. The bacteria can use the captured CO_2 to dissolve the rock and subsequently generate crystals of $CaCO_3$ in periods of lower humidity and/or CO_2. A tentative model for the formation of these grey spots, supported by scanning electron microscopy and transmission electron microscopy data, is proposed.

Introduction

Carbonate rocks represent the world's largest carbon reservoir, with direct implications for the global carbon cycle. Serrano-Ortiz *et al.* (2010, 2011) estimated that the subterranean CO_2 pool could represent more than half of the annual atmospheric sink. In addition, considerable CO_2 is sequestered in carbonate rocks forming karstic caves. Two processes, dissolution and precipitation, are involved in the mobilization of carbon in subterranean environments (Saiz-Jimenez, 1999; Cañaveras *et al.*, 2006). Cave microorganisms are able to induce precipitation of carbonates, via biomineralization processes (Cañaveras *et al.*, 2001; Cuezva *et al.*, 2009) and also dissolution processes due to the excretion of acids (Northup & Lavoie, 2001; Engel *et al.*, 2004). Recent understanding of the importance of microorganisms in many geological processes, including speleothem formation (secondary minerals deposited in a cave by the action of water), has led to increased interest in this field (Barton & Northup, 2007).

Evidence of microbial activity has been reported from caves in France (Bastian *et al.*, 2010), Italy (Groth *et al.*, 2001), Slovenia (Pašić *et al.*, 2010) and Spain (Schabereiter-Gurtner *et al.*, 2004; Saiz-Jimenez *et al.*, 2011). In some cases, bioinduced mineral formations have been described (Cañaveras *et al.*, 1999; Sanchez-Moral *et al.*, 2003).

Altamira is a well-studied cave in Cantabria, northern Spain (43°22′40″N, 4°7′6″W) (Fig. 1a). It is one of many caves in the upper vadose area of the tabular polygenic karstic system developed within Cretaceous bedrock. The cavity (270 m in length) is situated on a topographical high (152 m a.s.l.), and has a depth of 3–22 m (averaging 8 m) below the surface. The cave has one entrance, and a main passage varying from 2 to 12 m in height and 6 to 20 m in width. The thickness of the cover (host rock and soil) in most of the galleries varies between 4 and 10 m

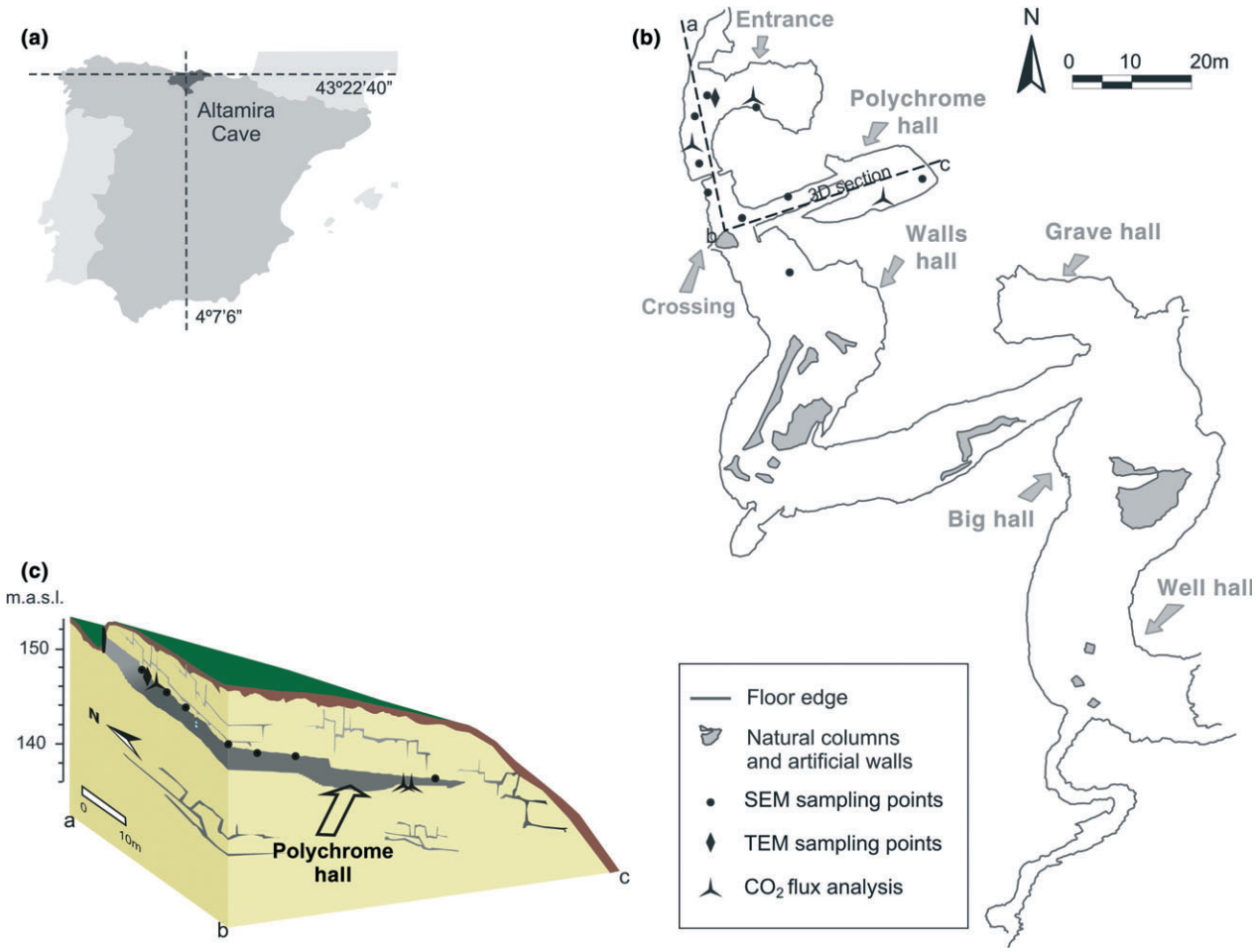

Fig. 1. (a) Geographical location of Altamira Cave (Cantabria, Spain). (b) Plan view of the cave with location of sampling points. (c) Idealized three-dimensional model of the cave area, as indicated in (b).

(see Fig. 1b and c). At present, the cave is permanently closed to visitors and thermally insulated from the outside through solid doors which also prevent the free circulation of air (Saiz-Jimenez *et al.*, 2011). Altamira Cave shows high thermohygrometric stability, relative humidity values near saturation and a pattern of strong seasonal shifts over the course of the year in terms of levels of trace gases. In summer, CO_2 concentrations are relatively steady near 500 μg g^{-1}, while winter concentrations are much higher and more erratic, sometimes exceeding 5000 μg g^{-1} (Cuezva *et al.*, 2011).

Altamira Cave has been the subject of intense microbiological and conservational studies for over a decade (Groth *et al.*, 1999; Sanchez-Moral *et al.*, 1999; Schabereiter-Gurtner *et al.*, 2002; Gonzalez *et al.*, 2006; Sanchez *et al.*, 2007; Cuezva *et al.*, 2009; Saiz-Jimenez *et al.*, 2011). These studies have concentrated on microbial communities growing on cave walls and ceiling. To the naked eye, these communities appear organized to form individual spots which are yellow, white or grey. In the present study, we focused on the grey spots and report the microbial community structure as well as the interactions between these microbes, the atmosphere and the underlying substratum.

Materials and methods

Sampling site and methodology

For microscopic studies, whole or parts of grey spots were sampled at four locations within the cave. These were at the Entrance Hall, Crossing, Polychrome Hall and Walls Hall (Fig. 1b and c). Sampling was carried out using sterilized scalpels. Sampled spots were collected in triplicate, stored in sterile tubes at 5 °C and analysed immediately upon arrival in the laboratory. Only samples collected from the Crossing (an area showing abundant and well-defined spots) were used to

extract environmental DNA; these were stored at −80 °C. Samples for transmission electron microscopy (TEM) were fixed *in situ* as specified below.

Microscopical and geochemical analysis

Textural and microstructural characterization of different grey spots was performed by environmental scanning electron microscopy (ESEM; Philips Quanta 200 with an Oxford EDAX detector) and SEM (Philips XL20; Oxford Instruments Analytical, UK). Energy-dispersive spectroscopy (EDS) analyses were performed using a Philips EDAX PV9900 with a light element detector type ECON. To improve photographic quality, the samples were metallized and observed under high vacuum conditions (Cañaveras *et al.*, 2001).

For TEM, small pieces of sample (1 mm diameter) were fixed with 2.5% glutaraldehyde in 0.1 M cacodylate buffer for 2 h. They were washed in the same buffer, postfixed in 1% osmium tetroxide, dehydrated in a graded acetone series and embedded in Spurr's resin. Ultrathin sections, cut from the block, were then stained with 2% uranyl acetate and lead citrate and examined using a JEOL 1010 TEM at 100 kV accelerating voltage.

Molecular techniques and sequence analysis

DNA extraction, PCR amplification of the 16S rRNA gene and cloning were performed as described elsewhere (Porca *et al.*, 2012; Supporting Information, Table S1). Only reactions involving bacteria-specific primers were successful and three 16S rRNA gene clone libraries were constructed. Inserts of a subset of 200 liquid-preserved clones were sequenced using primers 21F and 1492R at Macrogen Inc. (Seoul, Korea). Short sequences ($\leq$ 750 bp), sequences with an average quality score of $<$ 20 and putative chimeric sequences (chimera.slayer, Mothur software, Schloss *et al.*, 2009) were removed from the dataset. The remaining sequences were compared with those available in the GenBank (http://www.ncbi.nlm.nih.gov, BLASTN algorithm), GREENGENES (http://greengenes.lbl.gov, 'Compare' tool), Silva (www.arb-silva.de, 'Sina alignment' tool) and the Ribosomal Database Project (http://rdp.cme.msu.edu/, 'Classifier' tool) databases. Sequences were affiliated with a phylum if identity was $>$ 90% over the alignment length of $>$ 800 bp in different databases searched. The next-nearest cultivated species was obtained via the EZtaxon server (www.eztaxon.org) (Chun *et al.*, 2007). Operational taxonomic units (OTUs) at an evolutionary distance of 3% were defined in Mothur. The same software was used to compare microbial community structure (Libshuff function) and to calculate diversity indices. Diversity coverage was calculated using Good's formula (Good, 1953). The sequences were deposited in the EMBL database under accession numbers HE604266–HE604318.

Analysis of CO_2 effluxes from bacterial communities

For study of CO_2 effluxes from bacterial communities, a CO_2 automated analyser was used (Li-Cor 8100-102; Lincoln). This methodology is commonly used to measure CO_2 fluxes in soils (Marañón-Jiménez *et al.*, 2011). Experiments were performed in July 2010, when the CO_2 concentrations reach their yearly minimum (Saiz-Jimenez *et al.*, 2011). Measurements were taken at three different points: from the area abundantly covered by grey spots located on the wall of the Entrance Hall, and from two points of the ground sediments, observed to be free from grey spots with the naked eye, and located in the Entrance and Polychrome Halls (Fig. 1). At each measurement point we fixed and sealed with plastic putty (Terostat-81; Henkel, Heidelberg, Germany) a PVC collar (diameter 81.7 cm^2) on which the instrument chamber was placed. We performed three repetitions of 90 s each with 30-s intervals, measuring CO_2 (μmol per mol dry air) every second.

Results and discussion

Spatial distribution of grey spots

Grey bacterial spots growing inside Altamira Cave colonize different substrata, including limestone/dolostone host rock, calcite speleothems, pigmented areas and clays or cave sediments. The spots are 0.5–3.0 mm in diameter, roughly circular and show little relief. Morphologically, the spots differ in size and colour. Small spot morphotypes ($\leq$ 1 mm in diameter) are generally uniformly grey while large spot morphotypes (1.5–3.0 mm in diameter) tend to be darker grey. The intensity of the grey colour in large spots varies from spot to spot and even within one spot which often develop a lighter grey outer margin. Regardless of their size, grey spots are occasionally covered with water droplets.

The distribution of grey spots is shown in Fig. 2. Colonization density decreases progressively towards the interior of the cave (Saiz-Jimenez *et al.*, 2011). We chose to study the grey spots, which are particularly abundant at ceilings and walls of the halls and galleries close to the entrance. Unlike yellow spots (Cuezva *et al.*, 2009; Porca *et al.*, 2012) the grey spots contain large amounts of bioinduced crystals, and were thus the focus of study here.

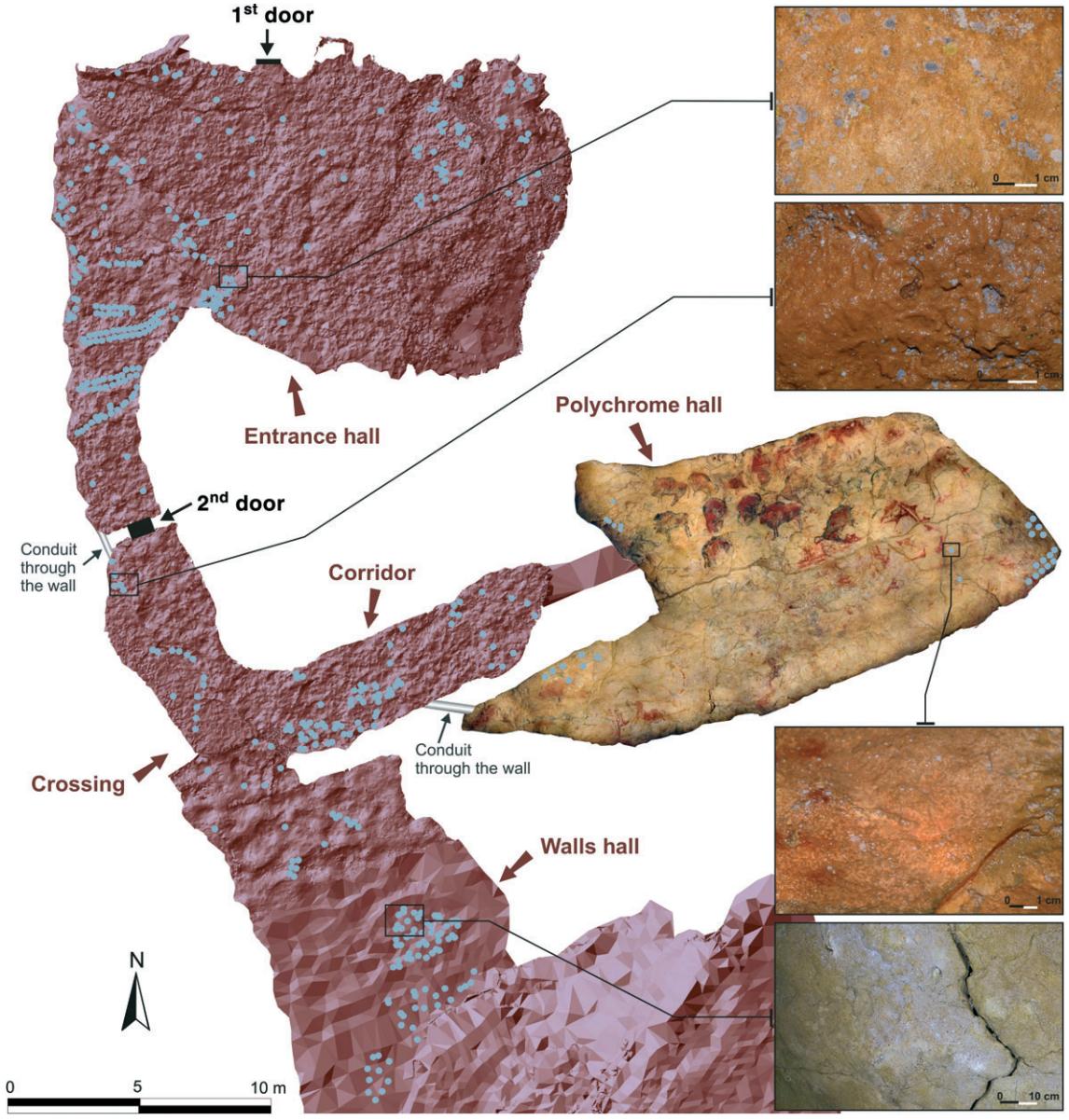

Fig. 2. Spatial distribution of microbial grey spots on the ceiling of the galleries and halls at Altamira Cave.

Spot structure and mineral biofabrics

Consistent with previous studies (Cuezva *et al.*, 2009), ESEM observations showed that the grey spots are formed by a dense network of microorganisms organized in well-defined branches, ranging in diameter between 10 and 30 μm. These have radial and dendritic divergent arrangements from the central area towards the exterior, producing a circular to irregular pattern (Fig. 3a and b). Morphologically, the microorganisms involved are mainly filamentous although coccoid forms are also observed. Furthermore, the branching is often embedded in extracellular polymeric substances (EPS).

Microbial growth was associated with two main types of $CaCO_3$ deposits (Fig. 3b–f). Nest or rosette-like fabrics comprise aggregates of subeuhedral to euhedral calcite crystals (2–4 μm in size) with radial arrangements and delineating an external pseudohexagonal contour. They usually have a central hole (0.5–0.7 μm in diameter) and generally rest on the substratum, often immersed within grey spots (or occasionally under them). The second type is represented by spheroidal or hemispheroidal elements averaging 8–10 μm in diameter and frequently reaching

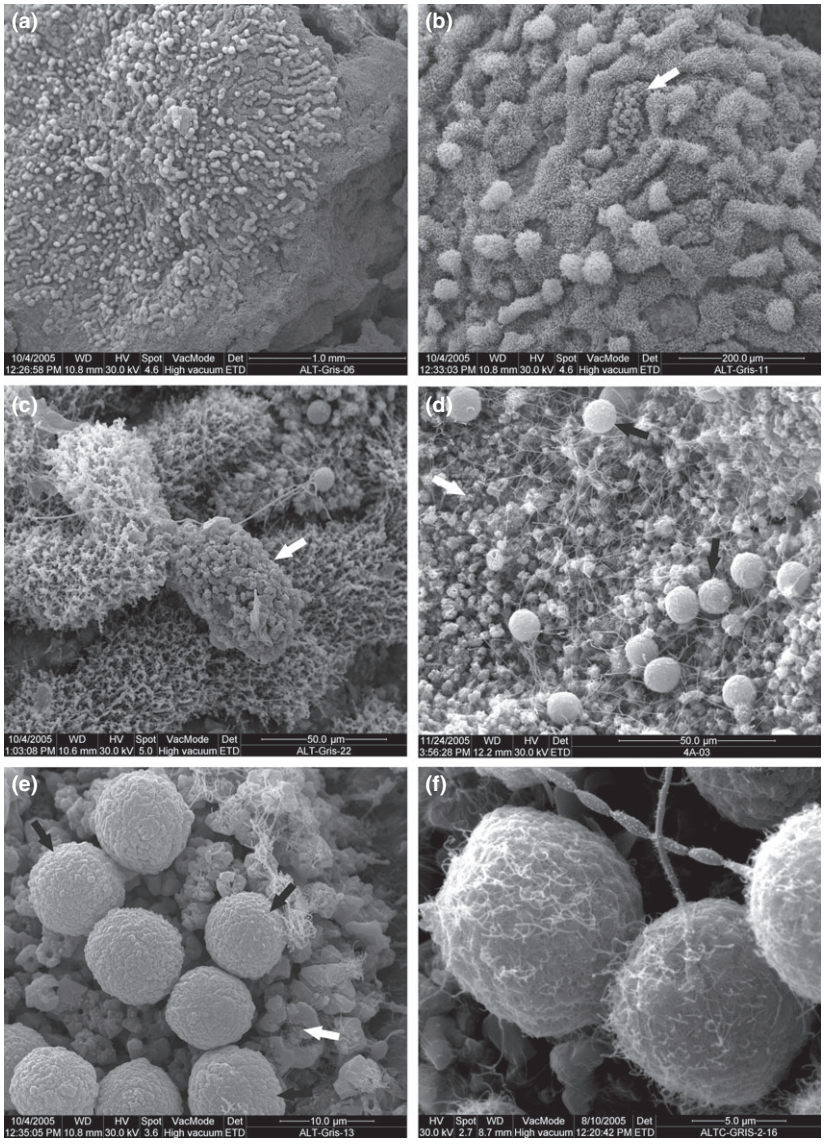

Fig. 3. Scanning electron micrographs of grey spots. (a) Grey spot showing radial and dendritic divergent arrangements from the central area towards the exterior. (b) Detail of a dense network of microorganisms organized in well-defined branches. A small patch of $CaCO_3$ nest-like aggregates with disperse spheroidal elements overlying is present in the spot (white arrow). (c) Small patch of $CaCO_3$ nest-like aggregates (white arrow) and filaments. (d) Continuous bed formed of $CaCO_3$ nest-like aggregates (white arrow) with dispersed spheroidal elements (black arrows). (e) Detail of spheroidal elements of $CaCO_3$ (black arrows) above a bed of $CaCO_3$ nest-like aggregates (white arrow). (f) Spheroidal elements of $CaCO_3$ coated with filamentous bacterial structures.

diameters up to 15 μm. On the surface, these elements are usually coated with bacterial structures (Fig. 3f). When not coated, these deposits are rhombohedral in shape (Fig. 3e), occasionally with slightly corroded crystal boundaries.

The level of mineralization differed with the size of the grey spot sampled. In the small morphotypes, spheroidal $CaCO_3$ deposits were scarce or even absent, while the rosette or nest-like aggregates generally formed small patches (Fig. 3a–c). In the large morphotypes, the $CaCO_3$ rosette or nest-like aggregates formed a thin continuous bed scattered with spheroidal elements (Fig. 3d). In spots showing a lighter grey outer zone, the mineral component was observed predominantly in the central zone, while the outer zone had a greater proportion of bacterial structures.

TEM transverse sections of grey spots revealed densely packed hyphae displaying several morphologies: filamentous and branched (cell diameter 120–240 nm) or globose (cell diameter 200–470 nm) (Fig. 4a–c).

The ultrastructural organisation of the cell wall displayed a series of layers typical of Gram-positive bacteria (Tetz *et al.*, 1993). All layers were involved in the formation of septum cross wall except for the outer cell-wall layer, which continued to surround the daughter cells (Fig. 4b).

The clustering of cells in tight groups appears to be a result of a particular division process during which the cells from the filament divide longitudinally leading to a new septum that then splits. From both sides of the split, new septa leading to the walls of the parent cell were often observed. This gives the appearance of a doughnut-

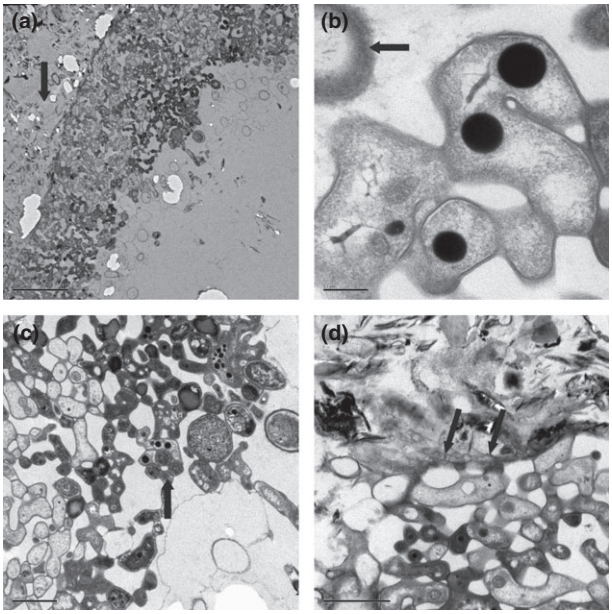

Fig. 4. Transmission electron micrographs. (a) Transverse section from the lateral side of a light grey spot. The substratum is on the left (arrow). (b) Hyphae divided transversely by cross walls but not separated into discrete units. On the upper left corner is an empty hypha with a shaggy outer border (arrow). (c) Cross and longitudinal sections through filamentous and globose hyphae. The hyphae in the middle form a network of doughnut-shaped appearance (arrow). (d) Hyphae penetrating into the underlying rock, thinning as they do so (arrows).

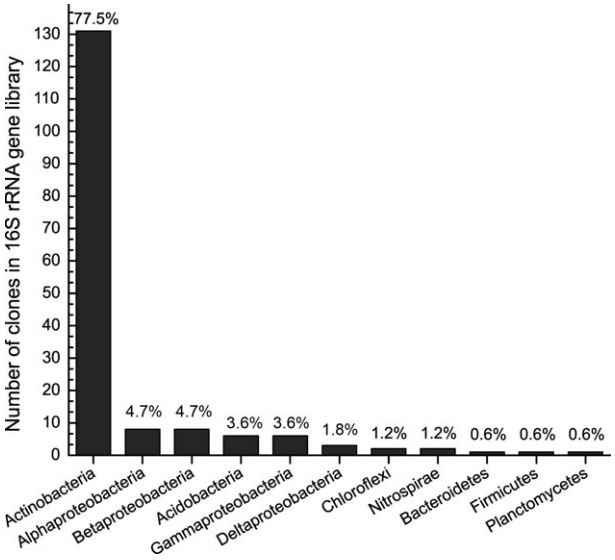

Fig. 5. Distribution of major phylogenetic groups in the 16S rRNA gene clone library constructed from environmental DNA obtained from the Altamira Cave grey spot samples.

shaped network (Fig. 4b and c). Some hyphae were able to penetrate into the underlying rock, becoming thinner as they did so (Fig. 4d). These hyphae ranged from 70 to 100 nm in diameter, which made them three to five times less voluminous than the average hypha in the spot.

The central depression of the spot contained a number of separate hyphae up to 1 μm that resembled isolated vesicles. These isolated round cells showed various degrees of degeneration and were even empty with a shaggy outer border (Fig. 4b). In all of them the structure of the membrane was still discernible.

Microbial community involved in the formation of grey spots

Total environmental DNA extracted from the three grey spot samples was used as template to amplify 16S rRNA genes of bacterial, archaeal or eukaryal origin. Only bacterial 16S rRNA gene sequences were successfully amplified, resulting in three 16S rRNA gene clone libraries. Sequences of 169 randomly chosen insert-positive clones met our quality criteria and were included in the final dataset. First, we compared the three individual clone libraries using Libshuff. This showed significant probability that the closest relative of each sequence is from the same community and the sequences were further considered as a single sample. Next, the sequences were grouped into OTUs at an evolutionary distance of 3%, a rough approximation to identify different bacterial species. This revealed 38 OTUs. We then estimated total diversity in the clone library by calculating ACE and Chao1 values. These were 155 (confidence interval 81–359) and 131 (confidence interval 72–293), respectively, much higher than the observed numbers of OTUs, indicating that further sampling would have revealed additional diversity. We finally calculated diversity coverage, representing the probability that a newly sampled sequence belongs to an already observed OTU (Good, 1953). The obtained value of 81.6% indicated that although rare taxa might remain undetected, the most common members of the community were detected in our library.

The sequences were assigned to phyla based on taxonomic affiliation of the closest relative (Fig. 5; Table S2). The analysed sample was strongly dominated by members of the *Actinobacteria*, which represented the vast majority (77.5%) of all environmental samples. Sequences affiliated with this phylum were followed in abundance only in the *Proteobacteria* (14.8% of all sequences sampled) while the remaining phyla detected appeared much less abundant and together represented 7.8% of the final dataset. Furthermore, the majority of actinobacterial sequences (75.7% of the final dataset) were most similar (85–99% 16S rRNA gene sequence similarity) to an environmental sequence recovered from a multicoloured cave-wall microbial community in Pajsarjeva jama, Slovenia (clone

3PJM80, FJ535092, Pašić *et al.*, 2010). The tools used in this study classified this abundant actinobacterial sequence group as belonging to the order *Nitriliruptoridae*. By contrast, levels of similarity between our sequences and recognized actinobacterial species were < 95% (82–92% to the nearest relative *Euzebya tangerina*), indicating that the predominant organisms involved in the formation of grey spots probably represent an unknown species.

Previous studies have indicated that a large number of bacteria are able to bioinduce $CaCO_3$ precipitation in caves (Cañaveras *et al.*, 2006). Laiz *et al.* (2003) found that 61% of the *Actinobacteria* isolated from Altamira Cave produced crystals in culture media. Attempts to isolate the bacteria involved in grey spot formation resulted in strains of the genera *Streptomyces* (some with grey mycelia) and *Bacillus* in this and in previous studies (Cañaveras *et al.*, 1999; Laiz *et al.*, 1999). In addition, members of these genera were found to induce $CaCO_3$ precipitation in Altamira Cave (Cañaveras *et al.*, 1999; Laiz *et al.*, 1999). Growth of these bacteria (which were not represented in the 16S rRNA gene clone library; Table S2) on agar medium can be explained by the refractory nature of the outer layer of the bacterial spore coat, which may prevent complete extraction of DNA (Riesenman & Nicholson, 2000).

The identification of *Streptomyces* and *Bacillus* agreed with previous works (Cañaveras *et al.*, 1999; Laiz *et al.*, 1999) suggesting that these genera were the main producers of $CaCO_3$ in Altamira Cave.

CO_2 effluxes from bacterial communities

This study represents a first attempt to test the usefulness of this methodology for cave microorganisms. According to the technical requirements of the CO_2 analyser system, the meteorological conditions in the cave were in the operating range of the instrument for the selected measured period.

Measurements of temporal variation of CO_2 carried out with the Li-Cor 8100 analyser system (Fig. 6) revealed differences in CO_2 effluxes (Fc) estimated at different sampling points. At the rock surface covered by grey spots the estimated Fc ranged from -0.53 to -0.60 μmol m^{-2} s^{-1} with good fit to a linear regression ($R^2 > 0.7$) indicating net CO_2 uptake. At the two measurement points with no visible grey spots, no significant CO_2 variation with time was measured (Fc = 0 μmol m^{-2} s^{-1}, $R^2 < 0.07$). Accordingly, CO_2 efflux measurements in an area heavily colonized by grey spots indicate that the bacterial communities involved have the ability to capture CO_2 from the air.

Several studies have linked the presence of carbonic anhydrase to bacterial uptake of atmospheric CO_2. Carbonic anhydrase is a zinc-containing enzyme that is widespread in the *Bacteria* domain and catalyses the reversible

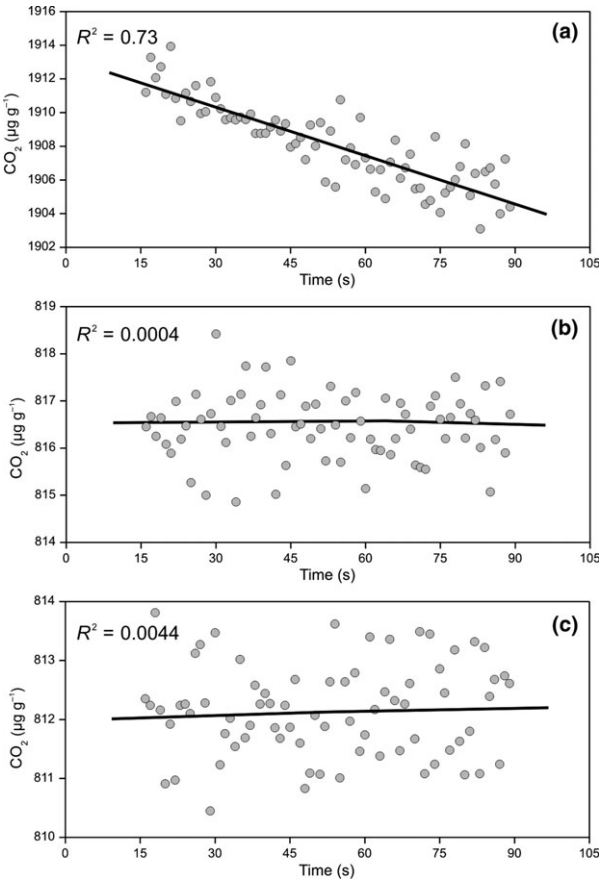

Fig. 6. Measurements of CO_2 variation with time (grey circles) at the three different sampling points: (a) in an area abundantly colonized by grey spots; (b,c) at two points of the ground sediments, free from grey spots (to the naked eye). The black line represents the line of linear regression.

hydration of CO_2. Zhang *et al.* (2011) considered the possibility that *Bacillus mucilaginosus* (*Firmicutes*) could capture atmospheric CO_2 through excreted carbonic anhydrase. We hypothesise that this enzyme might be responsible of the capture of atmospheric CO_2.

Mineral–microbe interaction processes and evolutionary model of grey spots

Figure 7 provides a tentative model of the interactions that exist between a grey bacterial spot and the environment. Bacteria could interact directly with the cave atmosphere by CO_2 uptake. On the other hand, bacteria interact with the overlying carbonate substratum via the chemical reactions that take place in the interface solution. Thus, the mineral–microbe interaction processes first depend on the uptake of CO_2 carried out by bacteria. CO_2 uptake causes a decrease in pH and subsequent dissolution of the limestone. Bacteria are therefore directly

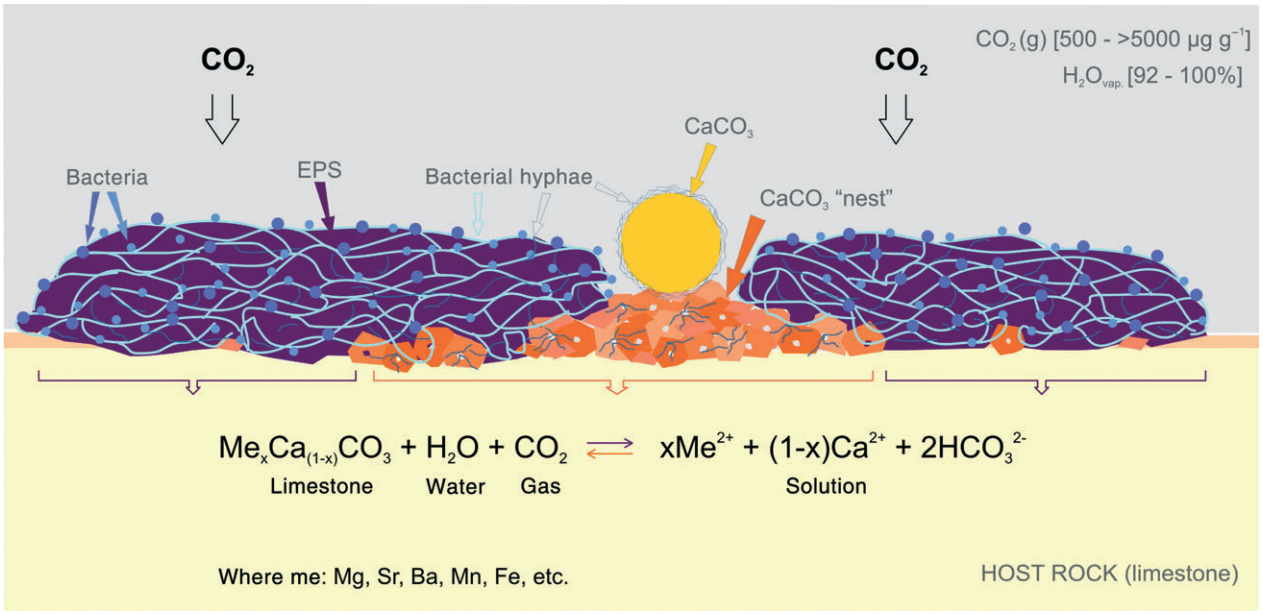

Fig. 7. Model of microbial–mineral interactions: section of a grey bacterial spot area overlying a limestone substratum.

responsible for the dissolution of the host rock. The release of Ca^{2+} in the solution that surrounds bacteria can result in mineral precipitation at periods of low CO_2 concentration in the cave air or of lower air humidity.

Observations on the origin and the variations on the microstructural elements and the microfabrics (SEM and TEM data) allowed us to propose an evolutionary model for grey spot formation based on the typology and distribution of the microorganisms, extracellular substances and minerals (Fig. 8).

Bacterial colonization phase

In the initial phase of grey spot formation airborne bacteria are deposited on the wet rock and cells attached to the substratum initiate colonization (Fig. 8a). This could explain the apparent isolation of spots. Bacterial colonization and their growth on the wet rock substratum results in the formation of a branching network of filamentous bacteria. The spot is light grey.

Settlement and proliferation of the grey spot

At the intermediate phase of grey spot formation the initial bacterial cells consolidate and generate further branching networks (Figs 3a,c and 8b). The spot consists of filamentous and coccoid bacteria and EPS, forming dendritic divergent branches. This coincides with the appearance of small and scattered deposits of aggregates or nests of rhomboedral crystals of $CaCO_3$. Some

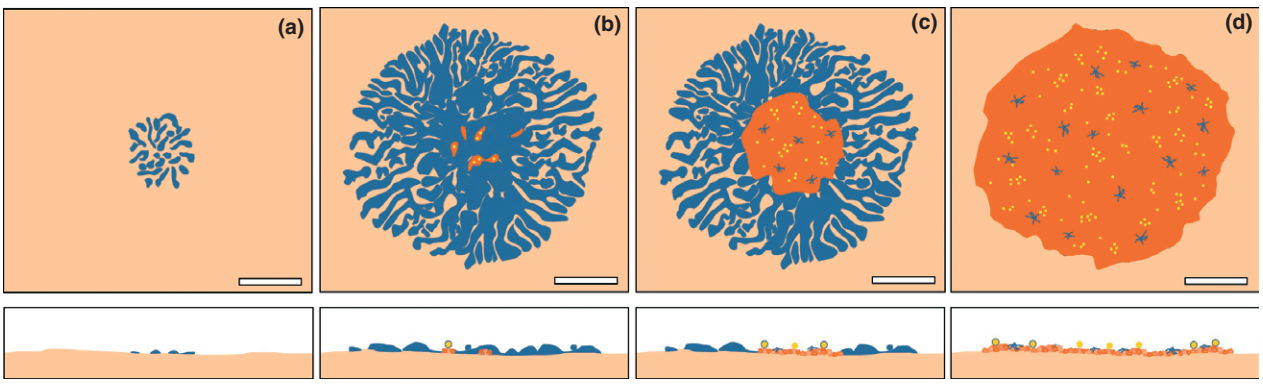

Fig. 8. Evolutionary model of grey spot formation. (a) Bacterial colonization phase; (b) settlement and proliferation of the spot; (c) advanced stage; (d) aged spot. Scale bar = 0.5 mm.

spheroidal $CaCO_3$ aggregates are further scattered above these deposits. The spot is light grey.

Advanced stage of grey spot

In a third developmental stage, the central area of the spot is dominated by the presence of $CaCO_3$ nests, rhomboedral crystals and scattered spheroidal elements (Figs 3d and 8c). The marginal zone of the spot again predominantly comprises divergent branches of filamentous and coccoid bacteria and EPS. This zonation is visible to the naked eye: the outer zone of the spot is light grey while the central area is dark grey.

Aged spot

In a final stage of development, biological structures have practically disappeared leaving only dispersed microbial filaments (Fig. 8d). The surface previously occupied by bacteria is now entirely covered with accumulated aggregates or $CaCO_3$ nests. Above these deposits, spheroidal elements of $CaCO_3$ are scattered, most of which are no longer coated with bacterial structures. The spot is uniformly dark grey.

Conclusions

Grey spots due to colonization of bacteria on the walls and ceiling of Altamira Cave from the entrance to the end of Polychrome Hall and at the beginning of Wall Hall are mainly formed by recognized or yet-to-be-cultivated *Actinobacteria* species which are able to capture CO_2 from the air and form calcium carbonate polymorphs. In particular, CO_2 efflux measurements in areas heavily colonized by bacteria indicate that they promote the uptake of this gas, which is very abundant in the cave (annual average about 3500 $\mu g\ g^{-1}$). This leads to dissolution of the rock substratum and the generation of $CaCO_3$ crystals as a by-product during periods of lower humidity and/or CO_2. In this context, the evolutionary model proposed for the formation of grey spots explains their wide variety of types. Future research should integrate stable carbon isotopic analyses to identify and quantify the origin of CO_2 effluxes at any given moment and the presence of carbonic anhydrase in the bacteria forming grey spots.

Acknowledgements

This research was supported by the Spanish Ministry of Science and Innovation, project CGL2010-17108 BTE and Consolider programme, project CSD2007-00058. S.C. was funded by a postdoctoral fellowship from the Spanish Ministry of Science and Innovation, research programme Juan de la Cierva. E.P. was supported by a CSIC JAE-Predoctoral grant. L.P. was supported by Slovenian Research Agency, research programme P1-0198. Altamira Cave Research Centre and Museum staff are thanked for their collaboration throughout the research period.

References

Barton HA & Northup D (2007) Geomicrobiology in cave environments: past, current and future perspectives. *J Cave Karst Stud* **69**: 163–178.

Bastian F, Jurado V, Novakova A, Alabouvette C & Saiz-Jimenez C (2010) The microbiology of the Lascaux Cave. *Microbiology* **156**: 644–652.

Cañaveras JC, Hoyos M, Sanchez-Moral S *et al.* (1999) Microbial communities associated to hydromagnesite and needle fiber aragonite deposits in a karstic cave (Altamira, Northern Spain). *Geomicrobiol J* **16**: 9–25.

Cañaveras JC, Sanchez–Moral S, Soler V & Saiz-Jimenez C (2001) Microorganisms and microbially induced fabrics in cave walls. *Geomicrobiol J* **18**: 223–240.

Cañaveras JC, Cuezva S, Sanchez-Moral S, Lario J, Laiz L, Gonzalez JM & Saiz-Jimenez C (2006) On the origin of fiber calcite crystals in moonmilk deposits. *Naturwissenschaften* **93**: 27–32.

Chun J, Lee JH, Jung Y, Kim M, Kim S, Kim BK & Lim YW (2007) EzTaxon: a web-based tool for the identification of prokaryotes based on 16S ribosomal RNA gene sequences. *Int J Syst Evol Microbiol* **57**: 2259–2261.

Cuezva S, Sanchez-Moral S, Saiz-Jimenez C & Cañaveras JC (2009) Microbial communities and associated mineral fabrics in Altamira Cave, Spain. *Int J Speleol* **38**: 83–92.

Cuezva S, Fernandez-Cortes A, Benavente D, Serrano-Ortiz P, Kowalski AS & Sanchez-Moral S (2011) Short-term CO_2(g) exchange between a shallow karstic cavity and the external atmosphere during summer: role of the surface soil layer. *Atmos Environ* **45**: 1418–1427.

DeLong EF (1992) *Archaea* in coastal marine environments. *P Natl Acad Sci USA* **89**: 5685–5689.

Diez B, Pedros-Alio C & Massana R (2001) Study of genetic diversity of eukaryotic picoplankton in different oceanic regions by small-subunit rRNA gene cloning and sequencing. *Appl Environ Microbiol* **67**: 2932–2941.

Engel AS, Stern LA & Bennett PC (2004) Microbial contributions to cave formation: new insights into sulfuric acid speleogenesis. *Geology* **32**: 369–372.

Gonzalez JM, Portillo MC & Saiz-Jimenez C (2006) Metabolically active Crenarchaeota in Altamira Cave. *Naturwissenschaften* **93**: 42–45.

Good IJ (1953) The population frequencies of species and the estimation of population parameters. *Biometrika* **40**: 237–264.

Groth I, Vetermann R, Schuetze B, Schumann P & Saiz-Jimenez C (1999) Actinomycetes in kartic caves of Northern Spain (Altamira and Tito Bustillo). *J Microbiol Methods* **36**: 115–122.

Groth I, Schumann P, Laiz L, Sanchez–Moral S, Cañaveras JC & Saiz-Jimenez C (2001) Geomicrobiological study of the Grotta dei Cervi, Porto Badisco, Italy. *Geomicrobiol J* **18**: 241–258.

Jurado V, Fernández-Cortes A, Cuezva S, Laiz L, Cañaveras JC, Sanchez-Moral S & Saiz-Jimenez C (2009) The fungal colonization of rock art caves. *Naturwissenschaften* **96**: 1027–1034.

Laiz L, Groth I, Gonzalez I & Saiz-Jimenez C (1999) Microbiological study of the dripping waters in Altamira cave (Santillana del Mar, Spain). *J Microbiol Methods* **36**: 129–138.

Laiz L, Gonzalez JM & Saiz-Jimenez C (2003) Microbial communities in caves: ecology, physiology, and effects on paleolithic paintings. *Art, Biology, and Conservation: Biodeterioration of Works of Art* (Koestler RJ, Koestler VR, Charola AE & Nieto-Fernandez FE, eds), pp. 210–225. The Metropolitan Museum of Art, New York.

Marañón-Jiménez S, Castro J, Kowalski AS, Serrano-Ortiz P, Reverter BR, Sánchez-Cañete EP & Zamora R (2011) Post-fire soil respiration in relation to burnt wood management in a Mediterranean mountain ecosystem. *For Ecol Manage* **261**: 1436–1447.

Northup DE & Lavoie KH (2001) Geomicrobiology of caves: a review. *Geomicrobiol J* **18**: 199–222.

Pašić L, Kovče B, Sket B & Herzog-Velikonja B (2010) Diversity of microbial communities colonising the walls of a Karstic cave in Slovenia. *FEMS Microbiol Ecol* **71**: 50–60.

Porca E, Jurado V, Žgur-Bertok D, Saiz-Jimenez C & Pašić L (2012) Comparative analysis of yellow microbial communities growing on the walls of geographically distinct caves indicates a common core of microorganisms involved in their formation. *FEMS Microbiol Ecol* DOI: 10.1111/j.1574-6941.2012.01383.x.

Riesenman PJ & Nicholson WL (2000) Role of the spore coat layers in *Bacillus subtilis* spore resistance to hydrogen peroxide, artificial UV-C, UV-B, and solar UV radiation. *Appl Environ Microbiol* **66**: 620–626.

Saiz-Jimenez C (1999) Biogeochemistry of weathering processes in monuments. *Geomicrobiol J* **16**: 27–37.

Saiz-Jimenez C, Cuezva S, Jurado V, Fernandez-Cortes A, Porca E, Benavente D, Cañaveras JC & Sanchez-Moral S (2011) Paleolithic art in peril: policy and science collide at Altamira Cave. *Science* **334**: 42–43.

Sanchez MA, Foyo A, Tomillo C & Iriarte E (2007) Geological risk assessment of the area surrounding Altamira Cave: a proposed natural risk index and safety factor for protection of prehistoric caves. *Eng Geol* **94**: 180–200.

Sanchez-Moral S, Soler V, Cañaveras JC, Sanz-Rubio E, van Grieken R & Gysels K (1999) Inorganic deterioration affecting the Altamira Cave, N Spain: quantitative approach to wall-corrosion (solutional etching) processes induced by visitors. *Sci Total Environ* **243/244**: 67–84.

Sanchez-Moral S, Cañaveras JC, Laiz L, Saiz-Jimenez C, Bedoya J & Luque L (2003) Biomediated precipitation of calcium carbonate metastable phases in hypogean environments: a short review. *Geomicrobiol J* **20**: 491–500.

Schabereiter-Gurtner C, Saiz-Jimenez C, Piñar G, Lubitz W & Rolleke S (2002) Altamira cave paleolithic paintings harbour partly unknown bacterial communities. *FEMS Microbiol Lett* **211**: 7–11.

Schabereiter-Gurtner C, Saiz-Jimenez C, Piñar G, Lubitz W & Rolleke S (2004) Phylogenetic diversity of bacteria associated with Paleolithic paintings and surrounding rock walls in two Spanish caves (Llonin and La Garma). *FEMS Microbiol Ecol* **47**: 235–247.

Schloss PD, Westcott SL, Ryabin T *et al.* (2009) Introducing mothur: open-source, platform-independent, community-supported software for describing and comparing microbial communities. *Appl Environ Microbiol* **75**: 7537–7541.

Serrano-Ortiz P, Roland M, Sanchez-Moral S, Janssens IA, Domingo F, Goddéris Y & Kowalski AS (2010) Hidden, abiotic CO_2 flows and gaseous reservoirs in the terrestrial carbon cycle: review and perspectives. *Agric For Meteorol* **150**: 321–329.

Serrano-Ortiz P, Roland M, Sanchez-Moral S, Janssens I, Domingo F, Goddéris Y & Kowalski AS (2011) Corrigendum to "Hidden, abiotic CO_2 flows and gaseous reservoirs in the terrestrial carbon cycle: review and perspectives". *Agric For Meteorol* **151-4**: 529.

Tetz VV, Rybalchenko OV & Savkova GA (1993) Ultrastructure of the surface film of bacterial colonies. *J Gen Microbiol* **139**: 855–858.

Zhang Z, Lian B, Hou W, Chen M, Li X & Li Y (2011) *Bacillus mucilaginosus* can capture atmospheric CO_2 by carbonic anhydrase. *Afr J Microbiol Res* **5**: 106–112.

Supporting Information

Additional Supporting Information may be found in the online version of this article:

Table S1. Targets, primers and PCR conditions used in this study.

Table S2. Affiliations of operational taxonomic units (OTUs) retrieved in this study and their distribution in the clone library constructed.

Please note: Wiley-Blackwell is not responsible for the content or functionality of any supporting materials supplied by the authors. Any queries (other than missing material) should be directed to the corresponding author for the article.